

Microfacies and geochemical evidence for original aragonite mineralogy of a foraminifera-dominated carbonate ramp system in the late Paleocene to Middle Eocene, Alborz basin, Iran

Mina Khatibi Mehr · Mohammad H. Adabi

Accepted: 3 July 2013 / Published online: 3 August 2013
© Springer-Verlag Berlin Heidelberg 2013

Abstract The Ziyarat Formation is a Late Paleocene to Middle Eocene carbonate sequence, located in the north of Tochal Village (south-east of Tehran). The Ziyarat Formation with a total thickness of 212.5 m conformably overlies the Fajan conglomerate and is overlain by greenish tuffaceous siltstone of the Karj Formation. Petrographic studies have led to the recognition of 11 microfacies. Of these microfacies, five belong to inner ramp, four belong to middle ramp and two are located in the outer ramp. Due to the great diversity and abundance of large benthic foraminifera (e.g., *Nummulites*, *Alveolina*, *Discocyclusina*), the Ziyarat Formation represents an example of “foraminifera-dominated carbonate ramp settings”. Paleobathymetry, light level and water energy were determined during deposition of Ziyarat carbonates based on the test shape and size variation of different types of benthic foraminifera and other components in different facies. Micritization, cementation, compaction, dissolution, dolomitization and fracturing are important diagenetic processes in the Ziyarat Formation, occurring in marine to meteoric and burial diagenetic environments. Geochemical studies indicate that Ziyarat carbonates were deposited in a shallow warm-water sub-tropical environment and aragonite was the original carbonate mineralogy with mean Sr values of 3,470 ppm. It should be noted that the maximum Sr content in abiotic calcite is 1,000 ppm. In Ziyarat limestone, dissolution as leaching is the most important diagenetic event in the evolution of porosity, particularly where *Nummulite* and

other benthic foraminifera are abundant. This may indicate that the original carbonate mineralogy of *Nummulites* might be aragonite, rather than low-Mg calcite. In the Jahrum Formation of Iran and in the El Garia Formation in north-east of Libya, the widespread moldic porosity in *Nummulite* beds enhanced the reservoir potential of the carbonate sequence. Thus, it is proposed that the original carbonate mineralogy of nummulitid shells may be varied in different environments, and those with metastable mineralogy are excellent for forming hydrocarbon reservoirs. Bivariate plots of Mn versus Sr/Ca and $\delta^{18}\text{O}$ values illustrated that Ziyarat limestones were affected by open diagenetic system with high water/rock interaction. Early burial diagenetic temperature calculation based on heaviest oxygen isotope values of micrite and δw of Eocene seawater of -0.85 SMOW showed that temperature was around 39°C . Cathodoluminescence studies of carbonate cements illustrated dull luminescence, because these carbonates were affected mainly by burial diagenesis. This statement is confirmed by $\delta^{18}\text{O}$ and $\delta^{13}\text{C}$ isotope evidences. Based on different facies and evidences such as absence of reefal facies, calciturbidite deposits, the occurrence of widespread tidal flat deposits and abundant micrites in all microfacies indicate that the Ziyarat Formation was deposited in a homoclinal carbonate ramp environment. In addition, many researchers suggested that due to extreme global warming during the Paleocene–Eocene time, platform margin coral reefs declined in low latitude and heterozoan calcitic foraminifers became abundant and, thus, widespread carbonate ramp systems developed.

M. Khatibi Mehr (✉) · M. H. Adabi
School of Earth Sciences, Shahid Beheshti University,
Evin, Velenjak Daneshjo Blv., Tehran, Iran
e-mail: minakhmehr@gmail.com

Keywords Ziyarat Formation · Microfacies · Sedimentary environment · Large benthic foraminifera · Geochemistry

Introduction

Nummulites and other large benthic foraminifera (LBF) such as *Assilina*, *Operculina* and *Alveolina* are abundant in Paleocene to Late Eocene carbonate sediments, particularly in shallow, oligotrophic, Circum-Tethyan platforms (Buxton and Pedley 1989). In the Middle East, nummulitic limestones form hydrocarbon reservoir and thus are potential exploration targets (Beavington-Penney et al. 2005). Larger Foraminifera cover a wide range of platform environments and are influenced by global and local factors such as temperature, water chemistry, nutrient, sea level and plate tectonics (Hallock and Glenn 1986; Hottinger 1997; Scheibner et al. 2005). Romero et al. (2002) proposed a model for the paleoenvironmental distribution of larger foraminifera based on late Middle Eocene deposits on the margin of the South Pyrenean basin. The Early–Middle Eocene was characterized by high atmospheric CO₂ content (mean ~ 900 ppmv; Zachos et al. 2001, 2008) and the warmest global temperature of the last 100 million years (Zachos et al. 2001). Payros et al. (2010) suggested that during the Middle Eocene time, the atmospheric buildup of greenhouse (CO₂) gases caused an increase in global temperature and eustatic sea-level rise. Increased atmospheric CO₂ concentrations will lead to ocean acidification and dissolution of aragonitic coral reefs. Increased sea-surface temperature causes zooxanthellae to be expelled from coral tissue, resulting in a decline in coral reefs and widespread mortality (Payros et al. 2010). For all these reasons, larger foraminiferal Eocene limestones have been regarded as analogs of future shallow water carbonate sedimentary environments if the ongoing global warming proceeds; thus, a reduction in carbonate platform fringing aragonitic coral reefs will occur (Hallock 2005; Pomar and Hallock 2008; Scheibner and Speijer 2008; Payros et al. 2010). Scheibner et al. (2005) also suggested that the larger foraminifer's turnover (LFT) during the Paleocene–Eocene transition closely correlated with the Paleocene–Eocene thermal maximum (PETM). Larger Eocene foraminifers were abundant when the Paleocene–Eocene hyperthermal global warming event caused severe environmental perturbations and, thus, a decline in fringing coral reef in the tropical shallow seas, because corals were particularly affected by extreme global warming (Schmitz and Pujalte 2007; White and Schiebout 2008; Payros et al. 2010). Therefore coral reefs in platform margin declined in low latitude warm water, and heterozoan calcitic foraminifers, better adapted to environmentally stressed conditions and thus widespread carbonate ramp systems developed (Hallock 2002; Pomar and Hallock 2008; Scheibner and Speijer 2008; Pujalte et al. 2009; Payros et al. 2010). A similar example has been reported from the Mesozoic extreme warming events due to intense volcanic CO₂ outgassing

(Jenkyns 2003) from the Aptian Oceanic Anoxic Event 1 (AOAE), in which photozoan carbonate characterized by coral and rudistids was replaced by a heterozoan agglutinated orbitolinid foraminifer (Burlar et al. 2008; Folmi and Gainon 2008). In all extreme greenhouse intervals, previous reef-rimmed carbonate platforms were replaced by gently dipping carbonate ramp systems, in which large benthic foraminifera were dominant (Payros et al. 2010).

The goals of this study are: to present the different types of microfacies, to interpret the depositional environment based on facies variations and morphology of foraminifers, and to determine the original carbonate mineralogy and different diagenetic processes.

Geological setting and stratigraphy

The type section of the Ziyarat Formation is located about 36 km south-east of Tehran, close to Tochal Village in Alborz Mountains, Iran (Fig. 1). The Ziyarat Formation was studied at 51°42'E, and 36°5'N. Tochal Village is located east of Anti-Alborz and is tectonically active. Thus, many major faults such as Tehran North, Qarehcheshmeh and North Tochal were recognized.

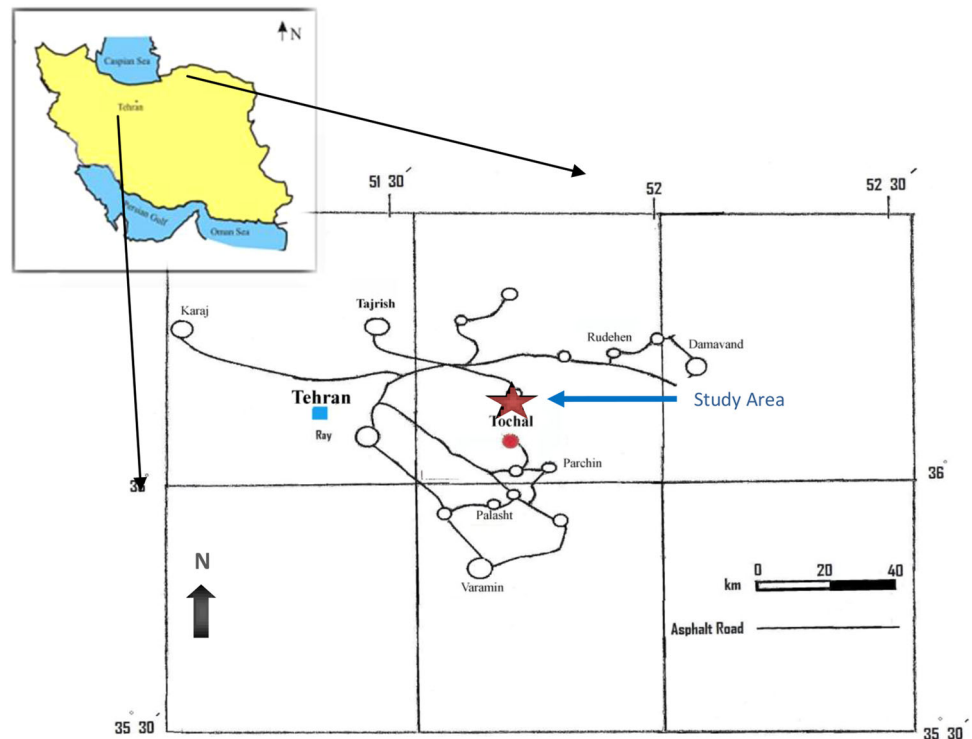
The Ziyarat Formation (Late Paleocene to Middle Eocene) was deposited as a local facies in Tochal Village. This formation has a total thickness of 212.5 m, conformably overlies the Fajan conglomerate and is overlain by greenish tuffaceous siltstone of the Karaj Formation. The age of the Late Paleocene–Middle Eocene was considered for the Ziyarat Formation at the type section, based on different foraminifera (Dellenbach 1964).

Stratigraphic sequences from base to the top of the formation consist of 13 m of finely laminated evaporates (gypsum), 65 m of finely laminated marl with gray to greenish color, 109 m of gray cliff forming thick bedded limestone and marly limestone, and finally 26 m of greenish limy marl (Fig. 2).

Methods

This study is based on 87 thin sections from samples collected near the type section of the Ziyarat Formation. Petrographic analysis was carried out on stained thin sections, using the method of Dickson (1965) to distinguish ferron and non-ferron calcite and dolomite. The petrographic classification for carbonates is based on Dunham limestone classification (Dunham 1962). Flügel (2004) facies belts were also used. Measurements of *nummulitid*, *alveolinid* and *operculina* size, as well as their test shapes [diameter/thickness (D/T) ratio] show variation along the paleoenvironmental gradient (Beavington-Penney et al. 2006).

Fig. 1 Location map of the study area in Alborz, Iran (Atlas road of Iran, Bakhtiyari 2011)



Twenty powdered samples (18 micrites and 2 samples from the test of *Nummulite*) were analyzed by atomic absorption spectrometer for Ca, Mg, Sr, Na, Mn and Fe at the Geology Department of the Shahid Beheshti University, Tehran, Iran, using 0.125 g samples. Because of low permeability of micrites, these samples are more reliable components for geochemical analysis (Asmerom et al. 1991; Adabi 2009). The precision was $\pm 0.5\%$ for Ca and Mg and ± 5 ppm for Sr, Na, Mn and Fe (Robinson 1980). Standard samples were used during elemental analysis to monitor the precision. Twelve powdered samples (eight micrites and four samples from test of *Nummulite*) which had previously been analyzed for major and minor elements were analyzed with a VG STRA Series II for oxygen and carbon isotopes at the Central Science Laboratory, University of Tasmania, Australia. Fifteen milligrams of powdered samples was allowed to react with anhydrous phosphoric acid in reaction tubes under vacuum at 25 °C for 24 h. The CO₂ extract from each sample was analyzed for $\delta^{18}\text{O}$ and $\delta^{13}\text{C}$ by mass spectrometry. The precision of data were established with duplicate analysis as $\pm 0.1\%$ for both $\delta^{18}\text{O}$ and $\delta^{13}\text{C}$, and these values were reported relative to PDB. Selected samples were observed with a cathodoluminescence microscope (Nikon CL, CCL 8200) at the Research Institute of Petroleum Industry (RIPI) in Tehran, Iran to determine different diagenetic sequences.

Facies analysis and depositional environment

Ziyarat carbonates consist of a large variety of skeletal and non-skeletal grains, calcite cements, micrites, and early and late diagenetic dolomites. Skeletal grains are mostly bivalves, crinoids, abundant benthic and some pelagic foraminifera, radiolitidae, red algae and bryozoan fragments. Miliolids, *Discocyclina* sp., *Actinocyclina* sp., *Astrocyclina* sp., *Operculina* sp., *Alveolina* sp. and *Rotalia* sp. are common and *Nummulites* sp. is the major type of benthic foraminifera in the Ziyarat Formation. Non-skeletal grains consist mainly of ooids, intraclasts and peloids.

Based on lithology, texture, sedimentary characteristics and association of benthic foraminifera, 11 shallow marine facies occur in the Ziyarat Formation. These facies consist of the inner carbonate ramp (including coastal tidal flat), the middle and the outer carbonate ramp facies belts. The characteristics of the inner and middle ramp facies belts are similar to those described in other Eocene carbonate ramps (Bassi 1998, 2005; Rasser 2000; Scheibner et al. 2003; Beavington-Penney and Racey 2004; Cosovic et al. 2004; Beavington-Penney et al. 2005; Rasser et al. 2005; Baratolo et al. 2007; Adabi et al. 2008; Payros et al. 2010; Racey et al. 2001). However, the outer ramp facies in this study are different with the Eocene storm dominated for algal ramp of the western Pyrenees described by Payros et al. (2010). In this study, an absence of calciturbidite

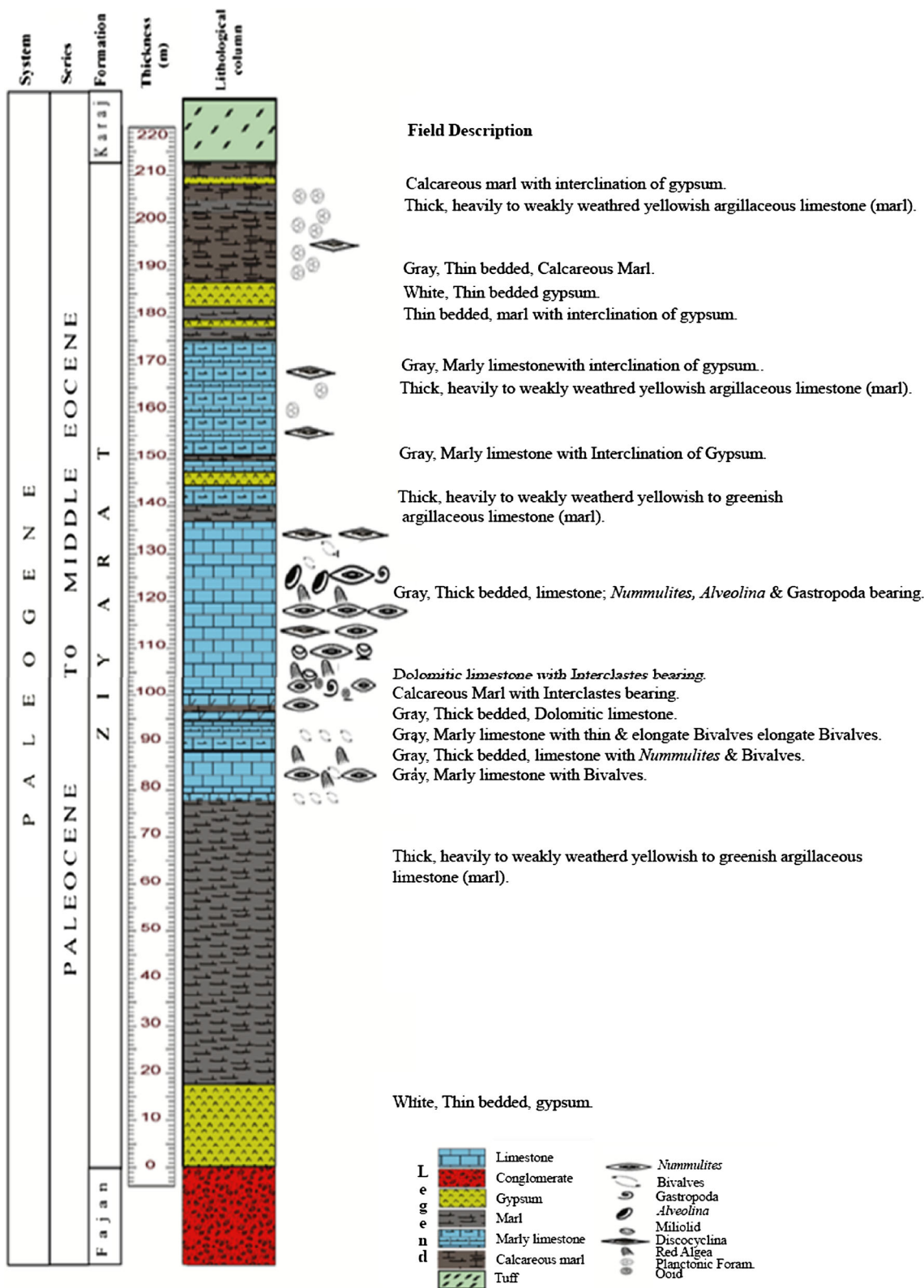


Fig. 2 Stratigraphic column of the Ziyarat Formation in the study area

deposits, reefal facies, gradual facies changes, widespread tidal flat deposits and abundant heterozoan calcitic foraminifers support that the microfacies in the Ziyart

Formation were deposited in a homocline carbonate ramp environment. Due to the great diversity and abundance of larger benthic foraminifera, this carbonate ramp is referred

to as a “foraminifera-dominated carbonate ramp system”. These microfacies are described briefly below from the shallowest to the deepest environment.

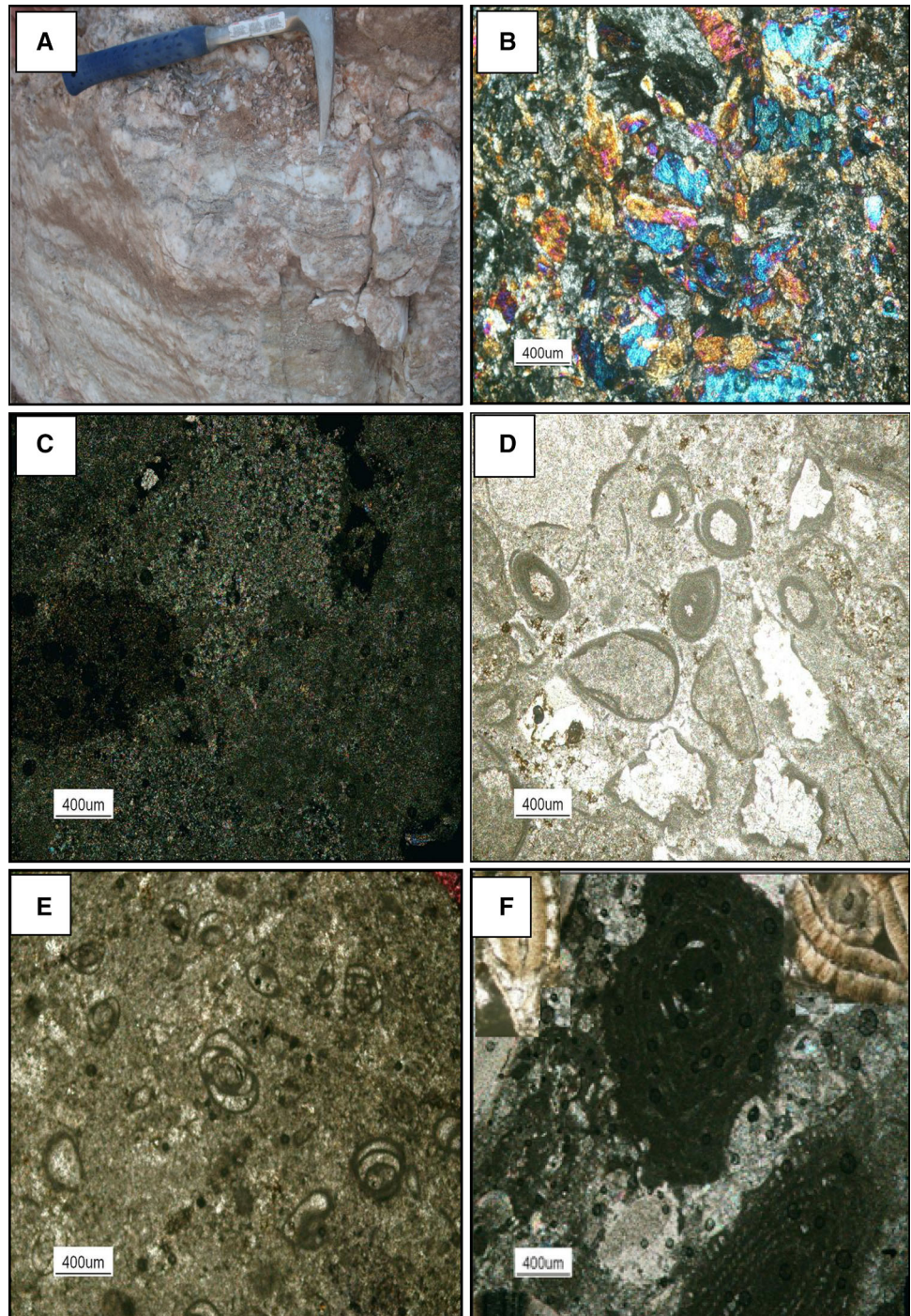
Inner ramp microfacies

Five microfacies were recognized in this sub-environment, composed mainly of evaporite, dolomicrite, intraclast, ooid and benthic foraminifera.

Evaporate facies

This facies consists of thin to thick bedded evaporite (Figs. 3a, b). Evaporite minerals and their pseudomorphs are common components of shallow marine carbonates. Evaporite has been defined as a rock that was originally precipitated from a saturated surface or near-surface brine in hydrological systems driven by solar evaporation (Warren 2006). The main site of modern marine sulfate

Fig. 3 **a** Evaporite facies in outcrop. **b** Evaporite fabric in thin section, W_A , XPL. **c** Dolomicrite or dolomudstone, $Z_{86.5}$, XPL. **d** Ooid intraclast packstone to grainstone, Z_{85} , PPL. **e** Miliolid wackestone, Z_{87} , PPL. **f** *Alveolina Nummulite* packstone, Z_{108} , XPL



precipitation is in the high intertidal and supratidal zones (Tucker 1991), where seawater is brought close to the surface by capillary action or from surface flooding (flood recharge).

In the Ziyarat Formation (Tochal section), evaporite sequence has a total thickness of 12.5 m. These evaporates are overlain by thick, heavily to weakly weathered yellowish to greenish argillaceous limestone (marl). Thin section studies of a few samples show that the crystals have low relief and weak birefringence, confirming gypsum mineralogy. Gypsum crystals in the form of swallow-tail twin crystals (Spencer and Lowenstein 1990) are present in many thin section samples. In addition, sulfate minerals in the Ziyarat Formation support the gypsum mineralogy, due to convincing structural evidence, such as chicken wire texture, to prove that these evaporates formed in subaerial dominated settings (such as coastal sabkhas). The sedimentary associations such as calcite pseudomorphs after evaporates, the lack of marine organisms (fossils), presence of bird's eye textures and few scattered fine silt-sized quartz grains within the micritic matrix may suggest that these evaporates formed in high intertidal to supratidal zones in a sabkha type of setting.

Dolomudstone

This microfacies consists mainly of dense, tightly packed, very fine to finely crystalline dolomite, ranging in size from less than 10 to about 16 μm (Fig. 3c). The presence of some traces of original depositional textures such as intraclasts, scattered silt- to sand-sized quartz grains, lamination, fenestral fabric, trace of calcite pseudomorph after evaporates and absence of fossil are the main features of this microfacies. On the basis of the above features, it is considered that this microfacies formed during very early diagenesis, under near-surface, low-energy condition, possibly in supratidal to intertidal sub-environments (Adabi 2009). These features indicate subaerial conditions, possibly in a zone with oscillating water table (Payros et al. 2010), with a subaerial exposure index higher than 60 % (Shinn 1983; Tucker and Wright 1990).

Ooid intraclast packstone to grainstone

The most common allochems in this microfacies include ooids and intraclasts (Fig. 3d). Ooids are commonly sub-spherical to sub-elongate, with mean size of 0.2 mm. Some ooids have undergone micritization, while others are affected by dissolution and therefore moldic porosity (oo-mold) is created. Intraclasts are generally polymodal in size, ranging from 0.2 to 0.4 mm with mean of 2.5 mm. Intraclasts are often rounded and are internally homogeneous and consist of micrites. The lack of bioclasts,

widespread dissolution features and relatively high quartz content indicate proximity to terrestrial source areas and suggest that this facies possibly formed in low- to high-energy environment, above fair-weathered wave base (FWWB) near coastal zone.

Miliolid wackestone

The predominant skeletal grains in this microfacies are miliolids ($\sim 25\%$). Other minor biogenic components include bryozoan fragments and red algae (Fig. 3e). Most foraminifera with imperforate porcelaneous wall (such as miliolids) suggest eutrophic condition, with increasing light level and high nutrient content. The high abundance of miliolids and the presence of a low-diversity foraminiferal association may be indicative of saline to hypersaline shallow marine conditions (Geel 2000). The presence of miliolids within mud matrix shows deposition in low-energy, shallow marine (lagoon) settings (Flügel 2004; Vaziri-Moghaddam et al. 2006; Brandano et al. 2009).

Alveolina Nummulite packstone

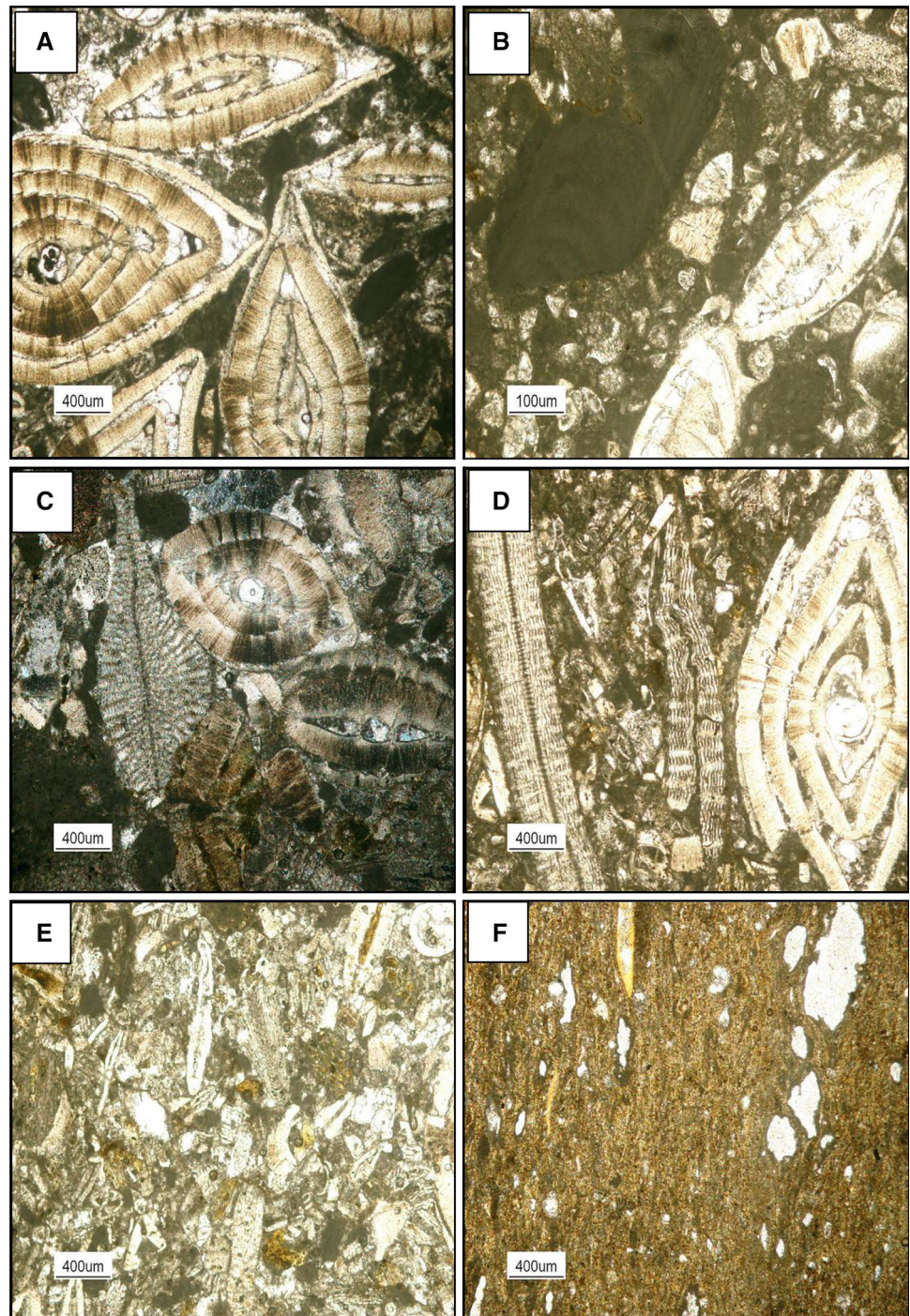
This microfacies is composed mainly of large benthic foraminifera, such as nummulitids (20–25 %) with mean size of 1.5 mm as well as porcelaneous alveolinids (10–15 %) (Fig. 3f). Other components include miliolids and green algae. *Nummulites* in this microfacies have robust to ovate test and thick shelled, indicating shallow low-energy marine environment with high light intensity and sufficient nutrients (Beavington-Penney and Racey 2004; Barattolo et al. 2007). This is supported by the dominance of the micritic matrix and abundance of alveolinids. The inner ramp environment is characterized by the predominance of mud-rich lithology with low-diversity faunal association, indicating a very shallow environment with low to moderate energy.

Middle ramp microfacies

Nummulite packstone

This microfacies is characterized by the dominance of nummulitids ($\sim 40\%$) (Fig. 4a). The other bioclastic components such as *Discocyclus* sp. and alveolinids are very rare, since alveolinids and *Discocyclus* thrive in different environments (Hohenegger et al. 1999; Adabi et al. 2008). The *Nummulites* are well preserved and the lack of abrasion of the *Nummulite* tests indicates that they were of autochthonous accumulation (Adabi et al. 2008). However, in some nummulitids tests breakage and re-orientation are present due to physical compaction.

Fig. 4 **a** *Nummulite* packstone, Z_{107.5}, PPL. **b** Red algal *Nummulite* packstone, Z₁₀₅, PPL. **c** *Discocyclus* *Nummulite* wackestone, Z₁₁₇, XPL. **d** *Nummulite* *Discocyclus* wackestone to packstone, Z₁₁₈, PPL. **e** Benthic foraminifera packstone, Z_A, PPL. **f** Radiolar sponge spicule wackestone, Z₁₄₁, PPL



Nummulitids thrived in oligotrophic (Langer and Hottinger 2000) to possibly slightly mesotrophic (Halfar et al. 2004) open marine environment, 40–80 m deep (Hottinger 1997; Beavington-Penney and Racey 2004). Micritic mud, chaotic fabric, scarcity of alveolinids and orbitolids in the matrix and general lack of sedimentary structures suggest nummulitid packstone deposited in a generally low-energy environment, below a fair-weather wave base (Scholle and Ulmer-Scholle 2006), (Adabi et al. 2008; Payros et al.

2010). Therefore, these facies are believed to represent the mid-ramp environment in which nummulitids flourished (Aigner 1985).

Red algal Nummulite packstone

This microfacies is dominated by the *Nummulites* (~ 32 %) and subordinate red algal fragments (~ 20 %). Other components are scarce *Discocyclus* sp., bryozoan

fragments, echinoid plates and small benthic foraminifers (e.g., rotaliids). *Nummulites* with both large- and small-sized tests are well preserved, but irregularly fragmented specimens also occur (Fig. 4b). Bioturbation structures are relatively high in this microfacies. Nummulitids was probably characterized by random scatter of nutrients or preferred lower nutrient level, while red algae tend to dominate in mesotrophic conditions (Bassi 2005). Red algae formed in oligophotic environments ~ 60 m deep, possibly near fair-weather wave base (Payros et al. 2010). Thus, the middle ramp was mostly located just below fair-weather wave base, at water depths between 40 and 80 m. This statement is very similar to that made by Barattolo et al. (2007) in Greece and by Bassi (2005) in northern Italy for Late Eocene middle ramp deposits, accumulated below fair-weather wave base.

Discocyclusina Nummulite wackestone

The predominant skeletal grains are lenticular nummulitids (~ 25 %) and orthophragminids (mainly *Discocyclusina* sp., *Actinocyclusina* sp. (Fig. 5a), *Asterocyclusina* sp. (Fig. 5b) and *Operculina* sp. (Fig. 5c) embedded in a mud matrix (Fig. 4c). Other components are echinoids, bryozoan fragments and alveolinids. No preferred particle orientation or imbricated fabric is present. The abundance of micritic

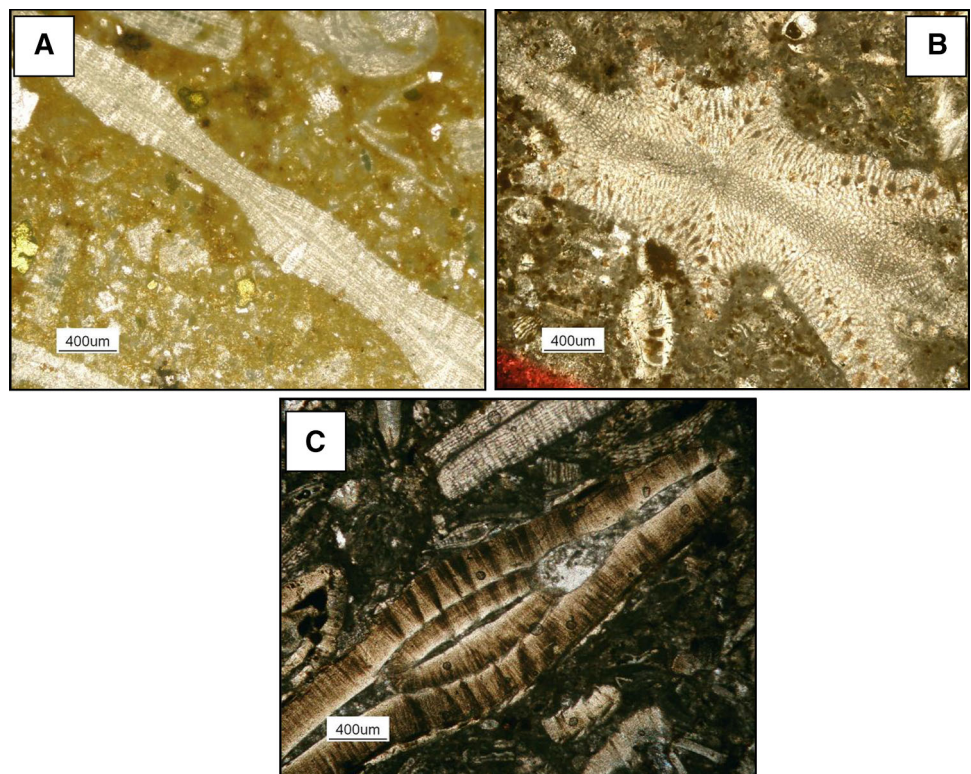
matrix and the fine-grained texture suggest a low-energy environment located below the fair-weather wave base.

Nummulite Discocyclusina wackestone to packstone

This microfacies is dominated by fragments of *Discocyclusina* (25–30 %), and *Nummulites* (20–25 %), (Fig. 4d). Some benthic foraminifera tests show breakage of their marginal cord. Most bioclasts are aligned parallel to the bedding plane. Elongated test shape, thinner test walls and abundance of mud matrix suggest that this microfacies deposited in much deeper oligophotic water, below fair-weather wave base (Pomar et al. 2004), because these organisms, with a mean D/T (e.g., diameter/thickness) ratio of 7.4, prefer decreasing light level and water energy (Rasser 2000; Beavington-Penney 2002). Thus, the sedimentary environment of this microfacies is in the deeper part of the middle ramp (Romero et al. 2002; Corda and Brandano 2003).

To sum up, the biotic assemblage presented mostly by nummulitids and discocyclusinids suggests sedimentation in the oligophotic zone of the middle ramp. The middle ramp in this study was mostly located just below the fair-weather wave base, at water depths between 40 and 80 m (Payros et al. 2010). This conclusion is very similar to that made by Bassi (2005) in northern Italy, Barattolo et al. (2007) in Greece and Payros et al. (2010) in the western Pyrenees

Fig. 5 **a** *Actinocyclusina* sp., Z₆₈, XPL. **b** *Asterocyclusina* sp., Z₁₂₀, PPL. **c** *Operculina* sp., Z₁₁₈, XPL



(Urbasa-Andia Formation) for Eocene middle ramp deposits, accumulated below the fair-weather wave base.

Outer ramp microfacies

Benthic foraminifera packstone

The predominant skeletal grains are (~ 40 %) fragments of *Nummulites* sp., *Discocyclus* sp., echinoids, brachiopods and thin pelecypod shells, belonging to open marine environment (Fig. 4e). Subordinate biogenic components include crinoid debris and sponge spicules. Abraded broken tests of *Nummulites* sp., *Discocyclus* sp., echinoids, brachiopods and thin pelecypod shells reflect prolonged hydrodynamic transport (Beavington-Penney and Racey 2004). There is no preferred bioclast orientation; a random, chaotic biofabric is very common. Quartz is generally absent in this facies.

Radiolar sponge spicule wackestone

The main components of this microfacies are sponge spicules (~ 12 %) and radiolaria (~ 10 %). The occurrence of radiolaria indicates that this microfacies belongs to the deepest part of the open marine carbonate ramp settings (Flügel 2004; Ghabeishavi et al. 2010; Adabi et al. 2010) (Fig. 4f). Light-independent and oligophotic organisms such as radiolarian indicate the deepest part of the photic zone, in the outer ramp area between 80 and 130 m (Hottinger 1997; Romero et al. 2002; Beavington-Penney and Racey 2004). The abundance of micritic matrix and the fine-grained texture show that current winnowing was mild suggesting a low-energy environment located below the fair-weather wave base and possibly below storm wave base. The most distinctive feature of the Ziyarat carbonate system was the outer ramp low-energy conditions (Table 1). In this microfacies, there is no evidence of current-induced imbricated fabric, grainstone facies or downslope-migrating sand wave by storm-induced currents described from a Miocene carbonate ramp from southern Spain by Puga-Bernabeu et al. (2010), from the Urbasa-Andia Formation (western Pyrenees) by Payros et al. (2010) and from the Eocene EL Garia Formation from Tunisia by Beavington-Penney et al. (2005). Thus, Ziyarat carbonates cannot be interpreted as a storm-dominated carbonate ramp.

Paleoenvironmental model

Eocene was a time of abundance of miliolid and larger benthic foraminifera (LBF), particularly nummulitids, alveolinids and *Discocyclus* sp. *Nummulites* occupied a

broad range of open marine environments on both ramp and shelf settings, and was generally absent from more restricted waters (Racey 2001). Smaller lenticular *Nummulites* occur in shallower, inner ramp/shelf settings, often along with alveolinids, whilst large flat *Nummulites* with similarly shaped *Assilina* and *Discocyclus* sp. occur in relatively deeper water (middle to outer ramp) environments (Beavington-Penney 2002; Vaziri-Moghaddam et al. 2006; Payros et al. 2010). Medium- to large-sized, lenticular to globular shaped *Nummulites* tend to occupy intermediate environments (Adabi et al. 2008). This broad pattern (with minor modification) is also presented in several studies of ancient ramps (e.g., Sinclair et al. 1998). The summary of key faunal associations on idealized carbonate ramp successions during the Eocene was suggested by Racey (1994). Based on this model, *Textulariids*, miliolids and *Orbitolites* occur in the shallowest, while *Discocyclus* sp. and *Assilina* occur in the deepest part of the ramp environment. This biotic association is typical of shallow, benthic calcareous communities in modern tropical to sub-tropical marine carbonate environment. Thus, larger foraminifers are valuable tools to construct paleoenvironmental models in the warm shallow marine settings (Geel 2000) and excellent indicators for facies interpretation (Rasser et al. 2005). The presence of larger foraminifera in the carbonate rocks of the Ziyarat Formation in Alborz shows the persistence of an equatorial climate throughout deposition of this formation, similar to other Tethyan carbonate platforms (Buxton and Pedley 1989).

Based on different microfacies associations recognized in the Late Paleocene to Middle Eocene of the Ziyarat Formation, a foraminifera-dominated gently dipping carbonate ramp model is proposed for this formation (Fig. 6). The larger foraminifers along with red algae (for algal deposits) were main carbonate producers in the Eocene shallow marine ramp setting throughout the world (Wilson and Vecsei 2005; Payros et al. 2010). The lack of any reefal development, absence of high-energy grainstone, gradual deepening trend from the shallow platform to the basin, no evidence of re-sedimentation, (e.g., calciturbidite) and the occurrence of abundant micrite in all microfacies are more compatible with a ramp setting than a shelf (Wright 1986; Tucker et al. 1993). This suggests a low-energy setting, which is more likely to occur on low-gradient slope characteristic of a ramp environment. The Ziyarat Formation in this study is separated into the inner ramp, the middle ramp and the outer ramp according to Burchette and Wright (1992). The inner ramp settings are characterized by alveolinid and miliolids dominated microfacies types, and middle ramp settings are dominated by nummulitids and discocyclusinids. The outer ramp settings consist mainly of Radiolaria and sponge spicules. In this study, there was no evidence of high-energy oceanic currents and strong storm

Table 1 Facies of the Ziyarat Formation

Facies	Characteristics	Interpretation
Inner ramp microfacies		
Evaporate facies	Evaporate minerals and their pseudomorphs are common components of shallow marine carbonates. These evaporates are overlain by thick, heavily to weakly weathered yellowish to greenish argillaceous limestone (marl)	Crystals have low relief and weak birefringence, confirming gypsum mineralogy. Gypsum crystals in the form of swallow-tail twin crystals (Spencer and Lowenstein 1990) are present in many thin section samples. Presence of bird's eye textures, and few scattered fine silt-sized quartz grains within the micritic matrix may suggest that these evaporates formed in high intertidal to supratidal zones in a sabkha type of setting
Dolomudstone	Consists mainly of dense, tightly packed, very fine to finely crystalline dolomite, ranging in size from <10 to about 16 μm	It is considered that this microfacies formed during very early diagenesis, under near-surface, low-energy condition, possibly in supratidal to intertidal sub-environments (Adabi 2009). These features indicate subaerial conditions, possibly in a zone with oscillating water table (Payros et al. 2010)
Ooid intraclast packstone to grainstone	Ooids are commonly sub-spherical to sub-elongate, with mean size of 0.2 mm. Some ooids are affected by dissolution and therefore moldic porosity (oomold) is created. Intraclasts are generally polymodal in size, ranging from 0.2 to 0.4 mm, with mean of 2.5 mm. Intraclasts are often rounded and are internally homogeneous and consist of micrites	The lack of bioclasts, widespread dissolution features and relatively high quartz content indicate proximity to terrestrial source areas and suggest that this facies possibly formed in low- to high-energy environment, above fair-weathered wave base (FWWB), near the coastal zone
Miliolid wackestone	The predominant skeletal grains in this microfacies are miliolids (~25 %). Other minor biogenic components include bryozoan fragments and red algae	Most foraminifera with imperforate porcelaneous wall (such as miliolids) suggest eutrophic condition, with increasing light level and high nutrient content. The presence of miliolids within the mud matrix shows deposition in a low-energy, shallow marine (lagoon) settings (Flügel 2004; Vaziri-Moghaddam et al. 2006; Brandano et al. 2009)
Alveolina <i>Nummulite</i> packstone	Composed mainly of large benthic foraminifera such as nummulitids (20–25 %) (robust to ovate test and thick shelled), with mean size of 1.5 mm as well as porcelaneous alveolinitids (10–15 %). Other components include miliolids and green algae	<i>Nummulites</i> in this microfacies have robust to ovate test and thick shelled, indicating shallow low-energy marine environment, with high light intensity and sufficient nutrients (Beavington-Penney and Racey 2004; Barattolo et al. 2007)
Middle ramp microfacies		
<i>Nummulite</i> packstone	This microfacies is characterized by the dominance of nummulitids (~40 %). The other bioclastic components, such as <i>Discocyclina</i> sp., and alveolinitids are very rare	Nummulitids thrived in oligotrophic (Langer and Hottinger 2000) to possibly slightly mesotrophic (Halfar et al. 2004) open marine environment. Micritic mud, chaotic fabric, scarcity of alveolinitids and orbitolinitids in the matrix and general lack of sedimentary structures suggest nummulitid packstone deposited in a generally low-energy environment, below FWWB (Adabi et al. 2008; Payros et al. 2010)
Red algal <i>Nummulite</i> packstone	It is dominated by the <i>Nummulites</i> (~32 %) and subordinate red algal fragments (~20 %). Other components are scarce <i>Discocyclina</i> sp., bryozoan fragments, echinoid plates and small benthic foraminifers (e.g., rotaliids). <i>Nummulites</i> with both large and small-sized tests are well preserved, but irregularly fragmented specimens also occur	Nummulitids were probably characterized by random scatter of nutrients or preferred lower nutrient level, while red algae tend to dominate in mesotrophic conditions (Bassi 2005). Red algae formed in oligophotic environments ~60 m deep, possibly near FWWB (Payros et al. 2010). Thus, the middle ramp was mostly located just below the fair-weather wave base
<i>Discocyclina</i> <i>Nummulite</i> wackestone	The predominant skeletal grains are lenticular nummulitids (~25 %) and orthophragminids (mainly <i>Discocyclina</i> sp.), <i>Actinocyclus</i> sp., <i>Asterocyclina</i> sp., and <i>Operculina</i> sp. embedded in a mud matrix	The abundance of micritic matrix and the fine-grained texture suggest a low-energy environment located below FWWB

Table 1 continued

Facies	Characteristics	Interpretation
<i>Nummulite</i> <i>Discocyclina</i> wackestone to packstone	This microfacies is dominated by fragments of <i>Discocyclina</i> (25–30 %), and <i>Nummulites</i> (20–25 %)	Elongate test shape and thinner test walls and abundance of mud matrix suggest that this microfacies deposited in much deeper oligophotic water, below the fair-weather wave base (Pomar et al. 2004). The biotic assemblage is presented suggesting that sedimentation in the oligophotic zone of the middle ramp, in this study was located just below FWWB (Payros et al. 2010)
Outer ramp microfacies	The predominant skeletal grains are (~40 %) fragments of <i>Nummulites</i> sp., <i>Discocyclina</i> sp., echinoids, brachiopods and thin pelecypod shells	These fragments of <i>Nummulites</i> sp. and <i>Discocyclina</i> sp. belong to open marine environment
Benthic foraminifera packstone Radiolar sponge spicule wackestone	The main components are sponge spicules (~12 %) and radiolaria (~10 %). The occurrence of radiolaria indicates that this microfacies belongs to the deepest part of the open marine carbonate ramp settings (Flügel 2004; Ghaibeishavi et al. 2010; Adabi et al. 2010)	Light-independent and oligophotic organisms such as radiolarian indicate the deepest part of the photic zone, in the outer ramp area between 80 and 130 m (Hottinger 1997; Romero et al. 2002; Beavington-Penney and Racey 2004)

waves suggested for a few Eocene carbonate ramp settings (e.g., Puga-Bernabeu et al. 2010; Payros et al. 2010). The biotic assemblage and paleolatitude of the Ziyarat Formation clearly suggest a tropical–subtropical depositional setting.

Foraminifera that live in shallow, wave-influenced environments exhibit ‘robust’, ovate tests with thick walls (decreasing D/T values), whilst tests from a facies deposited in much deeper, oligophotic water show increasing D/T ratio (i.e., flatter tests) and thinner test walls, reflecting decreased light levels and water energy at greater depths (Hallock and Glenn 1986; Beavington-Penney 2002). The test shape and wall thickness of the *Nummulites* and other LBF in the Ziyarat Formation along the paleoenvironmental gradient varied from inner to outer ramp sub-environment. In the inner ramp, the test shape is ovate with thick walls to prevent photo-inhibition of symbiotic algae within the test in bright sunlight and/or test damage in turbulent water. By increasing depth and decreasing sunlight and water energy, the test shape is elongate and flatter and test walls are thinner.

Diagenesis

The diagenetic processes that affected the Ziyarat carbonates were micritization, physical and chemical compaction, tectonic fracturing, cementation and dissolution (porosity development). Cementation and dissolution, which are discussed below, were the main diagenetic processes that affected the original texture, especially overprinting the porosity of this formation (Table 2).

Cementation

Different generations of sparry calcite cements were recognized in Ziyarat limestone, ranging from meteoric to burial cements. These include: clear syntaxial cements forming around echinoid fragments (Fig. 7a). These are the most common cements. Equant cements occur mainly as interparticle and sometimes within cavities (Fig. 7c). Vein calcite cements mostly occur throughout the limestone sequences as equant or platy fabric (Fig. 7e).

Dissolution

Porosity evolution

Dissolution is a destructive diagenetic process which increases porosity and permeability of the rocks and has major control on reservoir development (Moore 1989).

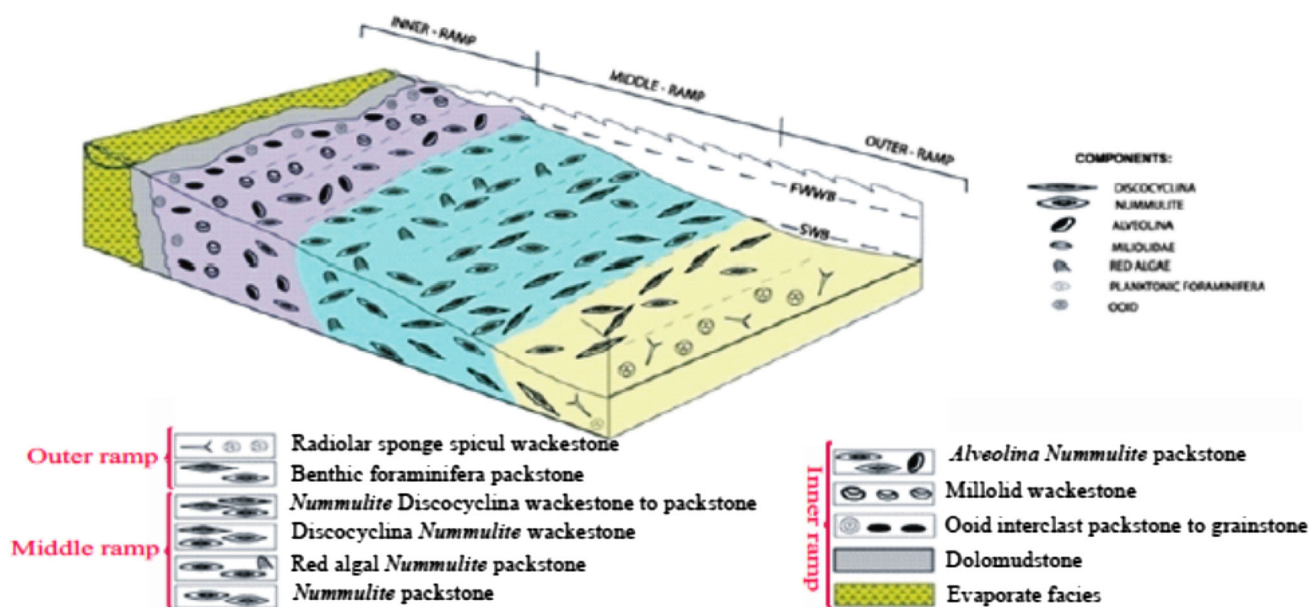


Fig. 6 Depositional model of a carbonates ramp platform of the Ziyarat Formation, Alborz Basin, Iran, and position of fair-weather wave base (FWWB); storm wave base (SWB)

Table 2 Paragenetic sequence of the Ziyarat Formation, Iran

Diagenetic	Early	Late
Bioturbation		
Boring & Micritization		
Geopetal Fabric		
Primary porosity (Intraparticle- Interparticle porosity)		
Dolomitization		
Equant cement		
Secondary porosity (Intercrystalline + Moldic + Vuggy + Channel & Fracture)		
Breakage & Deformation		
Clear syntaxial overgrowth cement		
Vein calcite cement		

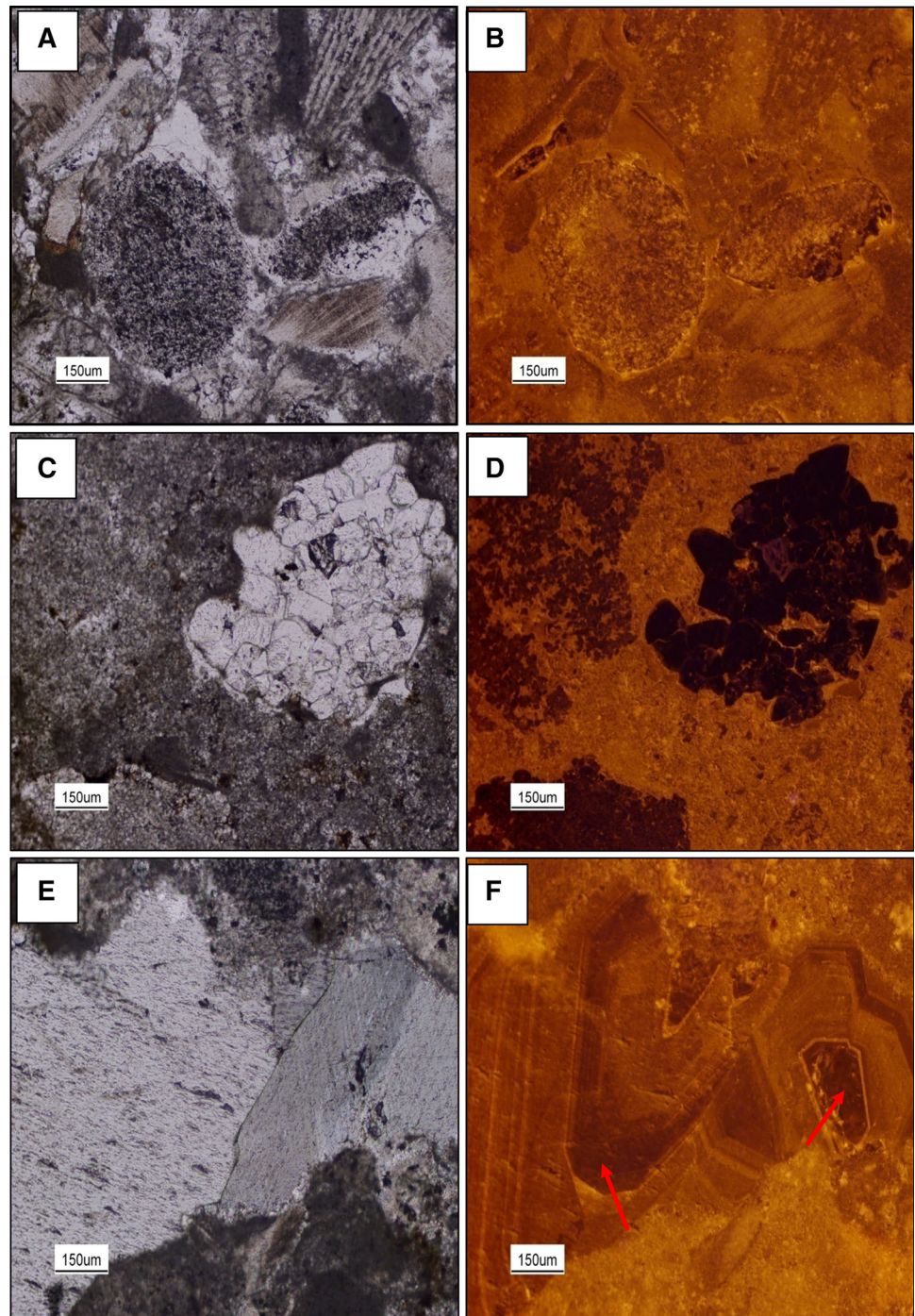
Dissolution in carbonates occur in near surface (vadose), phreatic and also burial diagenetic environment. In the Ziyarat Formation, dissolution as leaching is the most important diagenetic factor in the evolution of porosity, particularly in the inner to middle ramp facies. The primary porosity is very rare and the porous intervals exhibit mainly secondary porosity. The dominant porosity in this section is inter and intraparticle, moldic, vuggy and fracture types

(Fig. 8). Most of these porosities were filled by later stage calcite cements.

Discussion

Cathodoluminescence petrography illustrates that clear syntaxial cements are dull to non-luminescent (Fig. 7b),

Fig. 7 **a** Clear syntaxial overgrowth in Z_{103} , PPL; **b** same area as in **a** under cathodoluminescence. **c** Equant calcite cement as void filling in Z_{98} , PPL; **d** same area as in **c** under cathodoluminescence, indicating burial origin. **e** Coarse grain vein calcite cement, in Z_{102} , ppl; **f** same area as in **e** under cathodoluminescence. Vein calcite cement shows *bright yellow to brown* luminescence, possibly of meteoric origin, and *dark area (red arrow)* non-luminescence, indicating burial origin



indicating a burial origin (Tucker and Wright 1990). Under cathodoluminescence, the coarsely crystalline equant calcite cements are mostly of burial origin (Fig. 7d). Vein calcite cements are characterized by both bright luminescence to dull (dark) non-luminescence indicating meteoric and burial origin (Fig. 7f).

The porosity percentages and distributions are variable from minor (< 1 %) in the lower part of the section to common (between 1 and > 10 %) in the middle and upper

parts of the sections where *Nummulites* and other benthic foraminifera are abundant. This variation is facies controlled because it is lowest in outer ramp mud-supported facies. Thus, dissolution in grain-supported facies is a major control on the evolution of porosity in this study. Similarly, Moallemi (2010) showed that in the Jahrum Formation (Eocene in age) in Mond Oil Field in east of Busher (south-west of Iran), porosity is predominant in nummulitic facies as vuggy, intraparticle and moldic

Fig. 8 **a** Interparticle porosity in packstone sample, W1, XPL. **b** Intraparticle porosity in *Asselina* sp., Z_{107.5}, XPL. **c** Intercrystalline porosity in dolomite, Z_{66.5}, XPL. **d** Moldic porosity that filled with spary calcite, Z₈₅, XPL. **e** Vuggy to channel porosity in bioclast packstone, Z₁₁₈, XPL

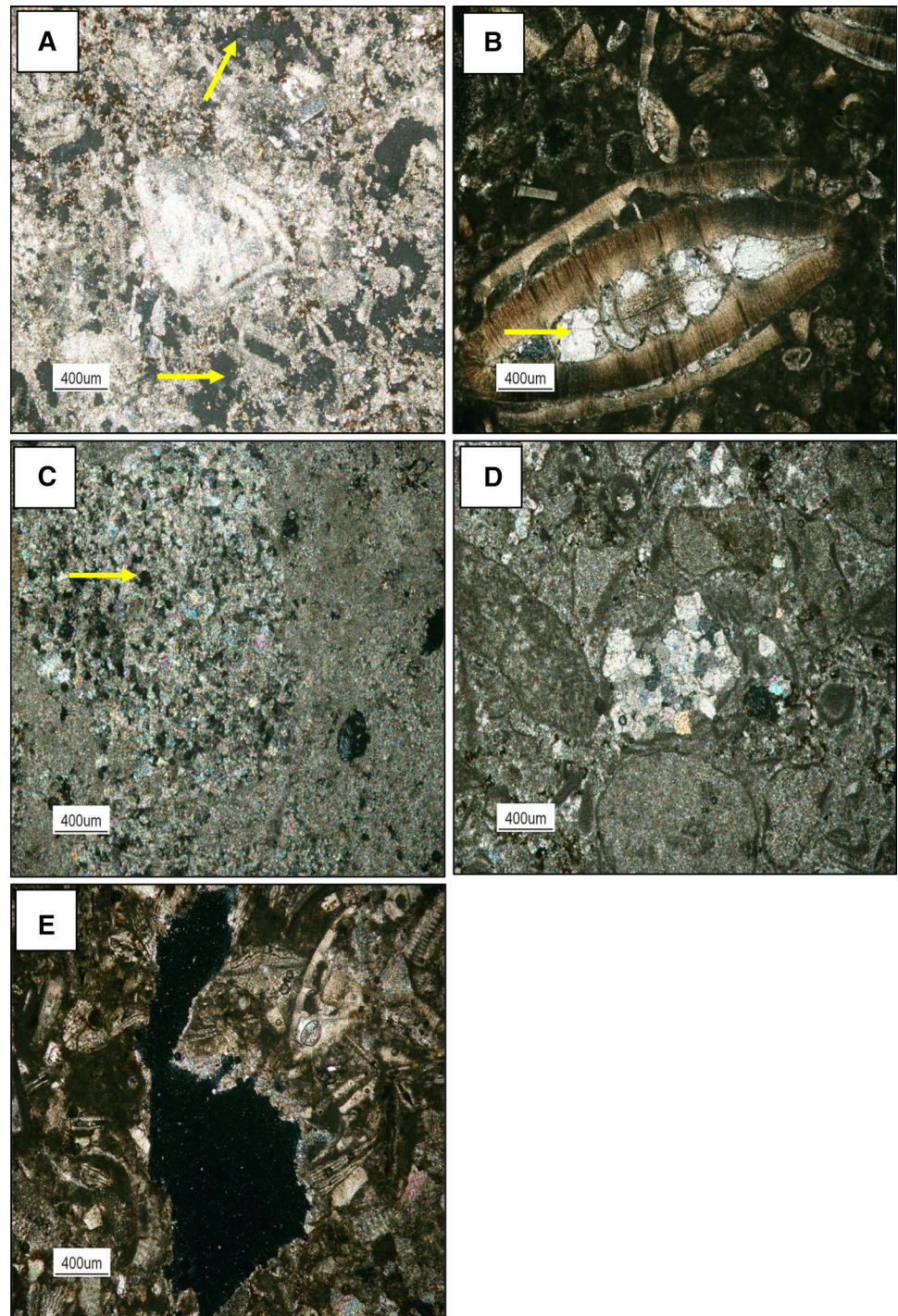


(Fig. 9; Moallemi 2010). Dissolution of nummulitic layers is the most important diagenetic event in the Jahrum Formation (Fig. 9). The widespread *Nummulite* beds with vuggy and moldic porosity, due to dissolution of benthic foraminifera, enhanced reservoir potential of the carbonate sequence in the Jahrum Formation.

In the El Garia Formation in north-east of Libya, *Nummulite* beds are partially to completely dissolved and

have major effect on porosity evolution and thus development of suitable hydrocarbon reservoirs (Jorry 2004). This may indicate that the original carbonate mineralogy of *Nummulites* might be aragonite/high-Mg calcite, rather than low-Mg calcite. It is proposed that the original carbonate mineralogy of *Nummulite* shells might be varied in different environments, and those with metastable mineralogy are excellent for forming hydrocarbon reservoirs.

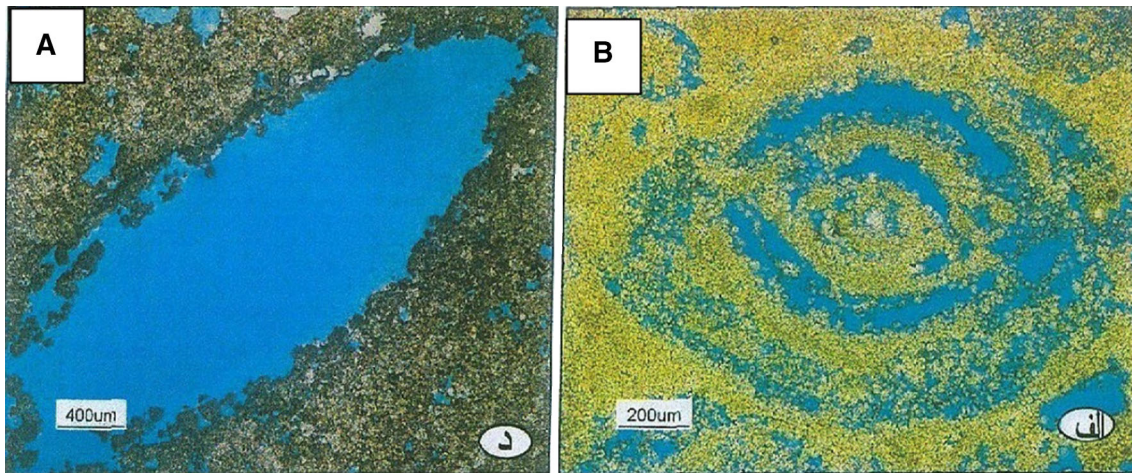


Fig. 9 a, b Moldic and intraparticle porosity in *Nummulite* tests in the Jahrum Formation, Gisakan Mountain and Mound #6 Oil Field, in East of Bushehr, Iran respectively. The blue color is due to injection of Epoxy resin, PPL (Moallemi 2010)

Bioturbation, boring and micritization, geopetal fabric, breakage and deformation are also present in different microfacies of the Ziyart Formation.

Determination of original carbonate mineralogy

Aragonite is the predominant mineral, along with some high-Mg calcite, forming in modern shallow sub-tropical warm waters (Milliman 1974; James and Clarke 1997). In modern temperate carbonates, high-Mg calcite predominates over low-Mg calcite, and in polar cold-water carbonates, low-Mg calcite is the dominant mineral (Rao 1981, 1996; Nelson 1988; Rao and Adabi 1992; James and Clarke 1997).

Studies of the original carbonate mineralogy during Phanerozoic was debated and discussed by many researchers (e.g., Sandberg 1983; Wilkinson et al. 1985; Wilkinson and Algeo 1989; Hardie 1996; Stanly and Hardie 1998; Dickson 2004). These workers have argued that the mineralogy of ancient carbonates may have been different from that of modern sediments, with calcite being considered the dominant mineral during the Ordovician, Devonian–mid-Carboniferous and Jurassic–Cretaceous to Early/Middle Cenozoic. However, some other researchers suggested that the assumption of change of original carbonate mineralogy through times needs to be re-evaluated (e.g., Nelson 1988; Rao 1991; Morse et al. 1997; Adabi 2004; Adabi and Asadi Mehmandosti 2008).

Determination of Ordovician Gordon Group sub-tropical shallow marine carbonates of Tasmania, Australia (Rao 1990); the Upper Jurassic carbonates (Mozduran Formation) in the Kopet-Dagh Basin in north-east Iran (Adabi and Rao 1991); the Cretaceous limestone of the Illam Formation in the Tange-Rashid area, Izeh, south-west of

Iran (Adabi and Asadi Mehmandosti 2008); the Lower Cretaceous carbonates (Fahliyan Formation), south-west Iran (Adabi et al. 2010), based on petrographic and geochemical evidences, indicates that aragonite, not calcite, was the dominant mineral in these warm-water sub-tropical carbonates. Recently, Westphal and Munneke (2003) also concluded that during Ordovician, Jurassic and Cretaceous periods, the original carbonate mineralogy was aragonite, similar to that of warm-water shallow marine carbonates.

In this study, petrographic, elemental and isotopic evidences were used to compare this information with modern aragonitic warm-water and calcitic cool to cold temperate carbonates and originally aragonitic mineralogy of Ordovician sub-tropical carbonates, the calcitic mineralogy of Permian sub-polar cold water of Tasmania, and the Upper Jurassic Mozduran carbonates of Iran to understand original carbonate mineralogy.

Geochemistry

Major and minor elements

Strontium The Sr concentration in recent tropical abiotic aragonite ranges from 8,000 to 10,000 ppm (Milliman 1974), whereas the maximum Sr contents in biotic calcite is 1000 ppm, without any diagenetic alteration (Adabi and Rao 1991; Rao 1996). The Sr contents increase with increase in aragonite content (Adabi and Rao 1991) and increase in water temperature (Morse and Mackenzie 1990). The concentration of Sr in Ziyarat limestone samples ranges from 383 to 3,472 ppm (mean 3,470 ppm) in micrite and from 1,026 to 1,092 ppm (mean 1,059 ppm) in the shell of *Nummulites* (Fig. 10a). Sr values of micritic samples show moderate diagenetic alteration, due to the replacement of aragonite by calcite during the two stages of

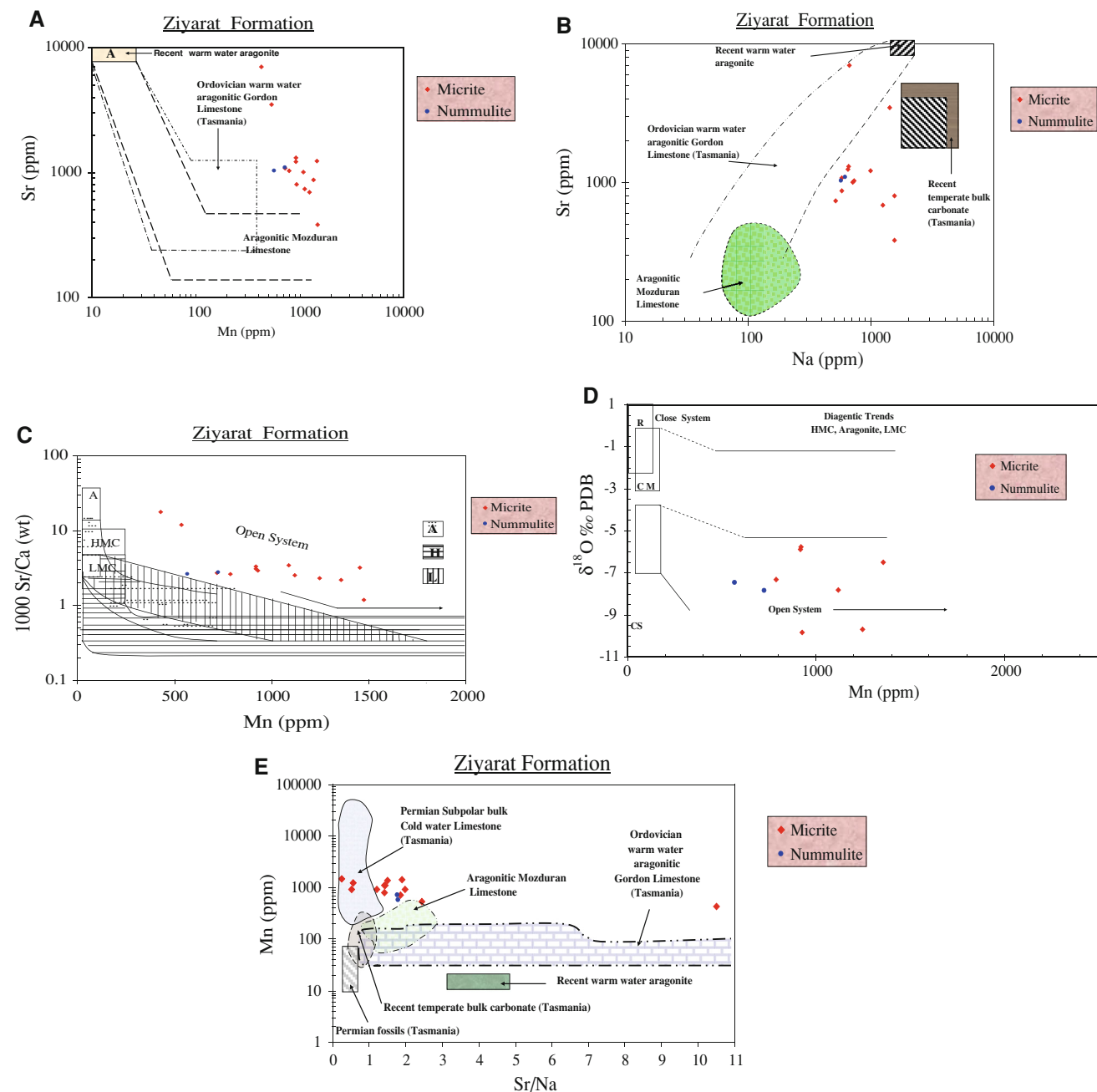


Fig. 10 **a** Sr and Mn variations in Ziyarat limestones, compared with fields of sub-tropical warm-water Ordovician aragonite (Rao 1991), Recent tropical shallow marine aragonite (Milliman 1974) and altered original aragonite mineralogy of the Mozduran Formation (Adabi and Rao 1991). **b** Sr and Na variations in Ziyarat limestones, compared with fields of recent temperate bulk carbonate (Rao and Adabi 1992; Rao and Ammini 1995), Recent tropical shallow marine aragonite (Milliman 1974), sub-tropical warm-water Ordovician aragonite (Rao

1991) and altered original aragonite mineralogy of the Mozduran Formation. **c** Sr/Ca versus Mn ratios in Ziyarat limestones. This trend shows that these carbonates were affected by non-marine fluids in an open diagenetic system (Brand and Veizer 1980). **d** Variation of $\delta^{18}\text{O}$ versus Mn also confirmed open diagenetic system. **e** Mn and Sr/Na variations in Ziyarat limestones. Note that the Sr/Na ratios of most samples are >1 , indicating the original aragonite mineralogy

diagenetic stabilization (Al-Aasm and Veizer 1986). The *Nummulite* shells have higher Sr value when compared with modern biotic calcite.

Sodium The Na concentration in recent tropical abiotic aragonite ranges from 1,500 to 2,700 ppm (mean

2,500 ppm; Land and Hoops 1973; Veizer 1983; Rao and Adabi 1992), whereas modern temperate calcitic sediments on have high mean Na content ($\sim 5,000$ ppm). The concentration of Na in carbonate sediments are related to salinity, biological fractionation, kinetics, mineralogy and

water depth (Land and Hoops 1973; Morrison and Brand 1986; Rao and Adabi 1992). The concentration of Na in the Ziyarat micrite samples ranges from 513 to 1,553 ppm (mean 911 ppm) and in shell of *Nummulites* from 572 to 619 ppm (mean 596 ppm). Na values are lower than those of modern warm-water aragonitic and calcitic counterparts, due to moderate diagenetic alteration. The plot of Sr–Na values shows that most limestone samples fall within or close to the warm-water sub-tropical aragonite fields of the Mozduran Formation (Adabi and Rao 1991) and the Gordon Group limestone of Tasmania, Australia (Rao 1991; Fig. 10b).

Manganese The concentration of Mn in Ziyarat limestone ranges from 430 to 1,475 ppm (mean 998 ppm) in micrites and 568 to 724 ppm (mean 646 ppm) in *Nummulite* tests. In modern warm-water aragonite, Mn and Fe concentrations are < 20 ppm (Milliman 1974), and in modern temperate shallow marine calcite sediments mean Mn is about 150 ppm (Rao and Adabi 1992). The higher Mn contents in both micrite samples and *Nummulite* shells, when compared with modern tropical and temperate carbonates, are due to diagenetic alteration by non-marine fluids. The Sr versus Mn values show that most samples fall close to the aragonite field of Mozduran and warm-water sub-tropical Gordon Group (Fig. 10a). The appreciable gain of Mn and loss of Sr and Na in these samples are due to high water/rock interaction in an open diagenetic system.

The bivariate plot of Sr/Ca versus Mn shows that the limestone samples have been stabilized by fluids in an open diagenetic system (Brand and Veizer 1980; Fig. 10c). Variation of $\delta^{18}\text{O}$ versus Mn (Fig. 10d) also confirmed the open diagenetic system.

Sr/Na ratio Modern and ancient tropical carbonates are differentiated from their non-tropical counterparts by their Sr/Na ratio and Mn contents (Rao 1991; Winefield et al. 1996; Adabi and Asadi Mehmandosti 2008; Adabi et al. 2010). Modern tropical aragonitic sediments have low Mn and high Sr/Na ratio from 3 to ~ 5 (mean 4); in contrast, modern temperate bulk carbonates have high Mn and low Sr/Na ratios < 1 to ~ 1 (Adabi and Rao 1991; Rao 1996, Fig. 10e). Sub-polar Permian cold-water fossils with calcite mineralogy and the Permian sub-polar bulk cold-water calcitic limestones have also an Sr/Na ratio of ~ 1 (Rao 1991, 1996). In the Ziyarat Formation, the mean Sr/Na ratio in both micritic samples and *Nummulite* shells is ~ 1.5 (Fig. 10e). This value is within the range of warm-water aragonitic carbonates. All the above evidences along with other petrographic and diagenetic features such as dissolution and evolution of porosity particularly in grain-supported facies, and presence of ooids, dolomites and evaporates support the interpretation that the original carbonate mineralogy of Ziyarat limestone was aragonite.

Oxygen and carbon isotopes

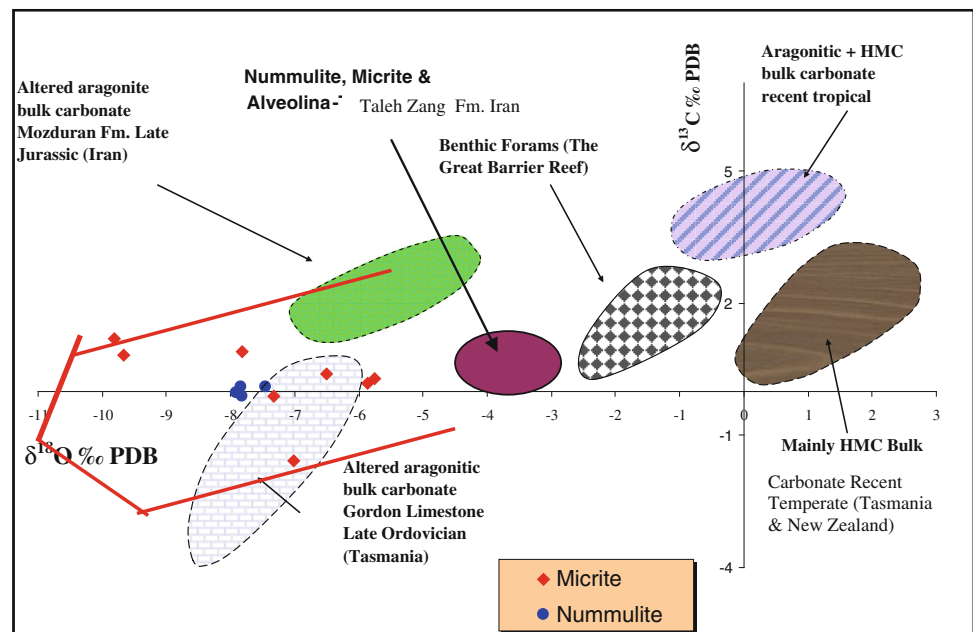
$\delta^{18}\text{O}$ and $\delta^{13}\text{C}$ are valuable tools for determination of paleotemperature, diagenetic trend, distinction between tropical, temperate and polar carbonates and recognition of the stratigraphic boundary between the two formations (e.g., Marshall 1992). The $\delta^{18}\text{O}$ values of the micritic samples of the Ziyarat Formation vary between -5.76 and -9.71 ‰ PDB (mean -7.73 ‰ PDB), and *Nummulite* shells ranges between -7.46 and -7.92 ‰ PDB (mean -7.69 ‰ PDB). The $\delta^{13}\text{C}$ values vary between $+1.2$ and -1.58 ‰ PDB (mean -1.39 ‰ PDB) in micrite samples and between -0.12 and $+0.1$ ‰ PDB (mean -0.11 ‰ PDB) in *Nummulite* shells. In Fig. 11, the isotope values of limestone samples have been compared with different isotopic carbonate fields, including recent warm shallow marine bulk carbonates (Milliman 1974), recent benthic forams of the Great Barrier reefs (Rao 1996), altered aragonitic carbonates of the Mozduran Formation (Adabi and Rao 1991), recent bulk temperate carbonates of Tasmania and New Zealand (Rao and Nelson 1992), altered micritic and benthic forams of Eocene deposits of the Tale-Zang Formation in Zagros Basin, south-west of Iran (Zohdi 2007) and altered aragonitic bulk carbonates of Gordon Limestone of Tasmania, Australia (Rao 1991). Most isotope data are plotted close or within isotopic field of altered aragonitic bulk carbonates of Gordon Limestone, probably due to similar original carbonate mineralogy and diagenetic system.

$\delta^{18}\text{O}$ versus $\delta^{13}\text{C}$ values from Ziyarat limestones indicate that diagenetic alteration occurred mainly in a burial diagenetic environment. The least-altered carbonate sample in this study, with a $\delta^{18}\text{O}$ value of -5.76 ‰ PDB, was used to calculate paleotemperature, using the equation of Anderson and Arthur (1983) and $\delta^{18}\text{O}$ value for Eocene seawater -0.85 ‰ SMOW (Veizer et al. 1999). This calculation gives an early shallow burial fluid temperature of about 39 °C.

Conclusions

1. The Ziyarat Formation is a shallow warm-water sequence of the Late Paleocene to Middle Eocene in age, overlies the Fajan conglomerate and is overlain by tuffaceous siltstone of the Karj Formation.
2. In the Ziyarat Formation, 11 microfacies were recognized from the distal to proximal part of the platform. of the 11 microfacies, 5 belong to the inner ramp, 4 to the middle ramp and 2 are located in the outer ramp settings. The lack of evidence of re-sedimentation, e.g., calciturbidite related to steep slope, absence of reefal facies and widespread tidal flat deposits, along with

Fig. 11 Comparison of $\delta^{18}\text{O}$ and $\delta^{13}\text{C}$ values of Ziyarat limestone samples with fields of recent calcitic temperate bulk carbonates (Rao and Adabi 1992), Recent warm shallow marine bulk carbonates (Milliman 1974), Eocene carbonate deposit of the Taleh-Zang Formation, Iran (Zohdi 2007), aragonitic Gordon Limestone of Tasmania, Australia (Rao 1991), aragonitic carbonates of the Mozduran Formation of Iran (Adabi and Rao 1991) and benthic forams of the Great Barrier reefs of Australia (Rao 1996)



abundance of large benthic foraminifera indicate that the Ziyarat Formation was deposited in a homocline carbonate ramp environment.

- The evaporite facies, dolomicrite, ooid intraclast packstone to grainstone, miliolid wackestone and *Alveolina Nummulite* packstone belong to the inner ramp, euphotic, sub-environment; the middle ramp microfacies, indicating an oligophotic zone, is composed of *Nummulite* packstone, red algae *Nummulite* packstone, *Discocyclusina Nummulite* wackestone and *Nummulite discocyclusina* wackestone to packstone; and outer ramp microfacies, showing the lower limit of the photic zone, consist of benthic foraminifera packstone and radiolar sponge spicule wackestone. *Nummulites* in the Ziyarat Formation show variation in test shape, along the paleoenvironmental gradient. *Nummulites* from the inner ramp have robust ovate shape with thick walls, while with increasing water depth and decreasing light levels, the test shape becomes flatter and elongate.
- Bivariate plots of minor elements such as Sr/Na versus Mn (~ 1.5), high Sr content in micritic facies (mean 3,470 ppm), along with petrographic studies (such as dissolution of nummulitic beds, leading to widespread moldic porosity) indicate that the original carbonate mineralogy was dominantly aragonite in Ziyarat limestone. This is in contrast with Payros et al.'s (2010) statement that increased atmospheric CO_2 concentrations lead to ocean acidification and dissolution of aragonitic coral reefs. We believe that the decline of coral reefs in the Eocene is mainly due to hyperthermal global warming event (not acidification of water), as corals are vulnerable to thermal stress, leading to a rise of heterozoan calcitic larger foraminifera (Hallock 2005). Larger foraminifera can tolerate high seawater temperatures and mesotrophic conditions (Hallock 2005; Pomar and Hallock 2008; Scheibner and Speijer 2008).
- Variations of Sr/Ca and also $\delta^{18}\text{O}$ values versus Mn suggest that diagenetic alteration occurred in an open system with high water/rock interaction.
- Variations of $\delta^{18}\text{O}$ and $\delta^{13}\text{C}$ values and CL studies of carbonate samples (dull to dark and typical yellow to orange luminescence) suggest that Ziyarat limestones were stabilized both in burial and meteoric diagenetic environment.
- Cementation and dissolution were the main diagenetic processes that affected the original texture, and especially overprinted the porosity of this formation. The porosity percentages and distributions are facies controlled, because they are lowest in the outer ramp mud-supported facies. The dominant porosity in this study is inter and intraparticle, moldic, vuggy and fracture types. Porosity is common in the middle and upper parts of the sections where *Nummulites* and other benthic foraminifera are abundant. The widespread moldic porosity in *Nummulite* beds enhanced reservoir potential of carbonate sequence in both Jahrum (Iran) and the El Garia (Libya) formations. This may indicate that the original carbonate mineralogy of *Nummulites* might be aragonite, rather than low-Mg calcite. Thus, it is proposed that the original carbonate mineralogy of nummulitid shells might be varied in different environments, and those with

metastable mineralogy are excellent for forming hydrocarbon reservoirs.

8. A temperature calculation based on the heaviest oxygen isotope value of the least-altered sample indicates that the early shallow burial diagenetic temperature was around 39 °C.

Acknowledgments The authors thank the School of Earth Sciences, Shahid Beheshti University, Iran, for elemental analysis, the Central Science Lab, University of Tasmania, Australia for isotope analysis, and Research Institute of Iranian Oil Company for CL Photomicrographs. We would also like to thank Mr Moradpour for CL photomicrographs, and Dr Abass Sadegi, Dr Ali Moallemi and Dr Massoud Lotfpour for their help in fossil identification and informative discussions.

References

- Adabi MH (2004) A re-evaluation of aragonite versus calcite seas. *Carb Evap* 19:133–141
- Adabi MH (2009) Multistage dolomitization of Upper Jurassic Mozduran Formation, Kopet- Dagh Basin, N.E. Iran. *Carb Evap* 24:16–32
- Adabi MH, Asadi Mehmandosti E (2008) Microfacies and geochemistry of the Ilam formation in the Tang-e Rashid area, Izeh, SW Iran. *Asian Earth Sci* 33:267–277
- Adabi MH, Rao CP (1991) Petrographic and geochemical evidence for original aragonitic mineralogy of Upper Jurassic carbonates (Mozduran Formation), Sarakhs area Iran. *Sediment Geol* 72:253–267
- Adabi MH, Zohdi A, Ghobishavi A, Amiri-Bakhtiyar H (2008) Applications of Nummulitids and other larger benthic foraminifera in depositional environment and sequence stratigraphy; an example from the Eocene deposits in Zagros Basin, SW Iran. *Facies* 54:499–512
- Adabi MH, Salehi MA, Ghabeishavi A (2010) Depositional environment, sequence stratigraphy and geochemistry of Lower Cretaceous carbonates (Fahliyan Formation), SW Iran. *J Asian Earth Sci* 39:148–160
- Aigner T (1985) Biofabrics as dynamic indicators in Nummulite accumulations. *Sediment Petrol* 55:131–134
- Al-Aasm IS, Veizer J (1986) Diagenetic stabilization of aragonite and low-Mg calcite, I. Trace element in rudists. *Sediment Petrol* 56:138–152
- Anderson TF, Arthur MA (1983) Stable isotopes of oxygen and carbon and their application to sedimentologic and paleoenvironmental problems. In: stable isotopes in sedimentary geology SEPM short course 10 section 1.1–1.151
- Asmerom Y, Jacobsen SB, Knoll AH, Butterfield NJ, Swett K (1991) Strontium isotopic variation of Neoproterozoic seawater: implication for crustal evolution. *Geochim Cosmochim Acta* 55:2883–2894
- Bakhtiyari S (2011) Atlas road of Iran, Geology department, p 320
- Barattolo F, Bassi D, Romero R (2007) Upper Eocene larger foraminiferal-coralline algal facies from the Klokova Mountain (south continental Greece). *Facies* 53:361–375
- Bassi D (1998) Coralline algal facies and their palaeoenvironments in the Late Eocene of northern Italy (Calcare di Nago, Trento). *Facies* 39:179–202
- Bassi D (2005) Larger foraminiferal and coralline algal facies in an Upper Eocene storm-influenced, shallow-water carbonate platform (Colli Berici, north-eastern Italy). *Palaeogeog Palaeoclimatol Palaeoecol* 226:17–35
- Beavington-Penney SJ (2002) Characterisation of selected Eocene Nummulites accumulations. PhD thesis, University of Wales, Cardiff
- Beavington-Penney SJ, Racey A (2004) Ecology of extant nummulitids and other larger benthic foraminifera: applications in palaeoenvironmental analysis. *Earth Sci Rev* 67:219–265
- Beavington-Penney SJ, Wright VP, Racey A (2005) Sediment production and dispersal on foraminifera-dominated early Tertiary ramps: the Eocene El Garia Formation, Tunisia. *Sedimentology* 52:537–569
- Beavington-Penney SJ, Wright VP, Racey A (2006) The Middle Eocene Seeb Formation on Oman: an investigation of acyclicity, stratigraphic completeness, and accumulation rates in shallow marine carbonate setting. *J Sediment Res* 76:1137–1161
- Brand U, Veizer J (1980) Chemical diagenesis of a multicomponent carbonate system- 1: trace elements. *J Sediment Petrol* 50:1219–1236
- Brandano M, Frezza V, Tomassetti L, Cuffaro M (2009) Heterozoan carbonates in oligotrophic tropical waters the Attard member of the lower coralline limestone formation (Upper Oligocene, Malta). *Palaeogeog Palaeoclimatol Palaeoecol* 274:54–63
- Burchette TP, Wright VP (1992) Carbonate ramp depositional systems. *Sediment Geol* 79:3–57
- Burlar S, Heinhofer U, Hochuli PA, Weissert H, Skeltone P (2008) Changes in sedimentary patterns of coastal and deep-sea successions from the North Atlantic (Portugal) linked to Early Cretaceous environmental change. *Palaeogeog Palaeoclimatol Palaeoecol* 257:38–57
- Buxton MWN, Pedley HM (1989) Short paper: a standardised model for Tethyan Tertiary carbonate ramps. *Geol Soc London* 146:746–748
- Corda L, Brandano M (2003) Aphotic zone carbonate production on a Miocene ramp. Central Apennines, Italy: *Sediment Geol* 161:55–70
- Cosovic V, Drobne K, Moro K (2004) Paleoenvironmental model for Eocene foraminiferal limestones of Adriatic carbonate platform (Istrian Peninsula). *Facies* 50:61–75
- Dellenbach J (1964) Contribution a l'etude geologique de la region situee a l'Est de Teheran. These University Strasbourg, p 120, 12 Pls., 43 Figs., 4 maps
- Dickson JAD (1965) A modified staining technique for carbonate in thin section: *Nature* 205:587
- Dickson S (2004) The arum Paris- continuum of mycorrhizal symbioses. *New Phytologist* article first published online: 163:187–200 [doi:10.1111/j.1469-8137.2004.01095.x](https://doi.org/10.1111/j.1469-8137.2004.01095.x)
- Dunham RJ (1962) Classification of carbonate rocks according to depositional texture. *Am Assoc Pet Geol Mem* 1:108–121
- Flügel E (2004) *Microfacies Analysis of Limestone: Analysis. Interpretation and Application*, Springer Verlag, Berlin, p 976
- Folmi KB, Gainon F (2008) Demise of the northern Tethyan carbonate platform and subsequent transition towards pelagic conditions: the sedimentary record of the Col de la Paline Morte area, central Switzerland. *Sediment Geol* 205:142–159
- Geel T (2000) Recognition of stratigraphic sequence in carbonate platform and slope deposits: empirical models based on microfacies analyses of Palaeogene deposits in southeastern Spain: *Palaeogeog Palaeoclimatol Palaeoecol* 155:211–238
- Ghabeishavi A, Vaziri- Moghaddam H, Taheri A, Taati F (2010) Microfacies and depositional environment of the Cenomanian of the Bangestan anticline. SW Iran: *J Asian Earth Sci* 37:275–285
- Halfar J, Godinez-Orta L, Mutti M, Valdez-Holguin JE, Borges JM (2004) Nutrient and temperature controls on modern carbonate

- production: an example from the Gulf of California, Mexico. *Geology* 32:213–216
- Hallock P (2002) Evolution and function of coral reefs. In: Cilek V (ed) *Earth system: history and natural variability*, in encyclopedia of life support system. Developed under the Auspices of the UNESCO, Eolss Publishers, Oxford. <http://www.eolss.net>
- Hallock P (2005) Global change and modern coral reefs: new opportunities to understand shallow-water carbonate depositional processes. *Sediment Geol* 175:19–33
- Hallock P, Glenn EC (1986) Larger foraminifera: a tool for paleoenvironmental analysis of Cenozoic depositional facies. *Palaios* 1:55–64
- Hardie LA (1996) Secular variation in seawater chemistry: an explanation for the coupled secular variation in the mineralogies of marine limestones and potash evaporates over the past 600 m.y. *Geology* 24:279–283
- Hohenegger J, Yordanova E, Nakano Y, Tatzreiter F (1999) Habitats of larger foraminifera on the reef slope of Sesoko Island, Okinawa, Japan. *Mar Micropaleontol* 36:109–168
- Hottinger L (1997) Shallow benthic foraminiferal assemblages as signals for depth of their deposition and their limitations. *Bull Soc Geol Fr* 168:491–505
- James NP, Clarke J (1997) *Cool-water Carbonates*. SEPM Spec Publ 56:440
- Jenkyns HC (2003) Evidence for rapid climate change in the Mesozoic–Palaeogene greenhouse world. *Phil Trans R Soc London A361*:1885–1916
- Jorry SJ (2004) *The Eocene Nummulite carbonates (Central Tunisia and NE Libya): sedimentology, depositional environments, and application to oil reservoirs*. PhD thesis, University of Geneva, Switzerland, p 120
- Kinsman DJJ, Holland HD (1969) The co-precipitation of cations with CaCO_3 . The co-precipitation of Sr^{2+} with aragonite between 16 and 96 °C. *Geochim Cosmochim Acta* 33:1–17
- Land LS, Hoops GK (1973) Sodium in carbonate sediments and rocks: a possible index to the salinity of diagenetic solutions. *J Sediment Petrol* 43:614–617
- Langer MR, Hottinger L (2000) Biogeography of selected “larger” foraminifera. *Micropaleontology* 46(supplement 1):105–126
- Marshall JD (1992) Climatic and oceanographic isotopic signals from the carbonate rock record and their preservation. *Geol Magazine* 129:143–160
- Milliman JD (1974) *Marine Carbonates*. Springer-Verlag, New York p 375
- Moallemi SA (2010) *Sedimentary environment and the effects of diagenetic factors in reservoir quality in Asmari- Jahrum Formation, East of Qatar Kazeron Fault (West of Coastal Fars), Iran* (PhD thesis) Shahid Beheshti University, p 316
- Moore CH (1989) *Carbonate diagenesis and porosity*. Elsevier, New York, p 338
- Morrison JO, Brand U (1986) Geochemistry of Recent marine invertebrates. *Geosci Canada* 13:237–254
- Morse JW, Mackenzie FT (1990) *Geochemistry of Sedimentary Carbonates*. Elsevier, New York p 707
- Morse JW, Wang Q, Tsio MY (1997) Influence of temperature and Mg:Ca ratio in the mineralogy of CaCO_3 precipitated from seawater. *Geology* 25:85–87
- Nelson CS (1988) An introductory perspective on non-tropical shelf carbonates. *Sediment Geol* 60:3–12
- Payros A, Pujalte V, Tosquella J, Orue- Etxebarria X (2010) The Eocene storm- dominated foralgal ramp of the western Pyrenees (Urbasa- Andia Formation): an analogue of future shallow-marine carbonate system? *Sediment Geol* 228:184–204
- Pomar L, Hallock P (2008) Carbonate factories: a conundrum in sedimentary geology. *Earth Sci Rev* 87:134–169
- Pomar L, Brandano M, Westphal H (2004) Environmental factors influencing skeletal grain sediment associations: a critical review of Miocene examples from the western Mediterranean. *Sedimentology* 51:627–651
- Puga-Bernabeu A, Martin JM, Braga JC, Sanchez-Almazo IM (2010) Downslope-migrating sandwaves and platform-margin clinoforms in a current-dominated, distally steepened temperate-carbonate ramp (Guadix Basin, southern Spain). *Sediment Geol* 57:293–311
- Pujalte V, Schmitz B, Baceta JJ, Orue-Etxebarria X, Bernaola G, Dinares-Turell J, Payros A, Apellaniz E, Caballero F (2009) Correlation of the Thanetian-Ilerdian turnover of larger foraminifera and the Palaeocene–Eocene thermal maximum: confirming evidence from the Campo area (Pyrenees, Spain). *Geol Acta* 7:161–175
- Racey A (1994) Biostratigraphy and palaeobiogeographic significance of Tertiary nummulitids (foraminifera) from northern Oman. In: Simmons MD (ed) *Micropaleontology and hydrocarbon exploration in the Middle East*. Chapman and Hall, London, pp 343–370
- Racey A (2001) A review of Eocene Nummulite accumulations: structure, formation and reservoir potential. *Petrol Geol* 24:79–100
- Racey A, Bauley HW, Beckett D, Gallagher LT, Hampton MJ, McQuilken J (2001) The petroleum geology of the Early Eocene El Garia Formation, Hasdrubal field, offshore Tunisia. *J Petrol Geol* 24:29–53
- Rao CP (1981) Criteria for recognition of cold-water carbonate sedimentation: Berriedale Limestone (Lower Permian), Tasmania, Australia. *Sediment Petrol* 51:491–506
- Rao CP (1990) Petrography, trace elements and oxygen and carbon isotopes of Gordon Group carbonate (Ordovician), Florentine Valley, Tasmania, Australia. *Sediment Geol* 66:83–97
- Rao CP (1991) Geochemical differences between subtropical (Ordovician), temperate (Recent and Pleistocene) and sub polar (Permian) carbonates, Tasmania, Australia. *Carb Evap* 6:83–106
- Rao CP (1996) *Modern Carbonates, Tropical, Temperate, Polar*. Introduction to sediment and geochemistry, Hobart (Tasmania), p206
- Rao CP, Adabi MH (1992) Carbonate minerals, major and minor elements and oxygen and carbon isotopes and their variation with water depth in cool, temperate carbonates, western Tasmania, Australia. *Mar Geol* 103:249–272
- Rao CP, Ammini ZZ (1995) Faunal relationship to grain-size, mineralogy and geochemistry in recent temperate shelf carbonates, western Tasmania, Australia. *Carb and Evap* 10:114–123
- Rao CP, Nelson CS (1992) Oxygen and carbon isotope fields for temperate shelf carbonates from Tasmania and New Zealand. *Mar Geol* 103:273–286
- Rasser MW (2000) Paleocology and Taphonomy of *Polystrata alba* (red algae) from the Late Eocene Alpine Foreland: a new tool for the reconstruction of sedimentary environments. *Palaios* 16(6): 601–607
- Rasser MW, Scheibner C, Mutti M (2005) A paleoenvironmental standard section for Early Ilerdian tropical carbonate factories (Corbieres, France; Pyrenees, Spain). *Facies* 51:217–232
- Robinson P (1980) Determination of calcium, magnesium, manganese, strontium and iron in the carbonate fraction of limestones and dolomites. *Chem Geol* 28:135–146
- Romero J, Caus E, Rossel J (2002) A model for the palaeoenvironmental distribution of larger foraminifera based on Late Middle Eocene deposits on the margin of the south Pyrenean basin (SE Spain). *Palaeogeog Palaeoclimatol Palaeoecol* 179:43–56
- Sandberg PA (1983) An oscillating trend in Phanerozoic nonskeletal carbonate mineralogy. *Nature* 305:19–22

- Scheibner C, Speijer RP (2008) Decline of coral reefs during late Paleocene to early Eocene global warming. *Earth Sci Rev* 3:19–26
- Scheibner C, Reijmer JGG, Marzouk AM, Speijer RP, Kuss J (2003) From platform to basin: the evolution of a Paleocene carbonate margin (Eastern Desert, Egypt). *Int Earth Sci* 92:624–640
- Scheibner C, Speijer RP, Marzouk AM (2005) Turnover of larger foraminifera during the Paleocene–Eocene Thermal Maximum and palaeoclimatic control on the evolution of platform ecosystems. *Geology* 33:493–496
- Schmitz B, Pujalte V (2007) Abrupt increase in seasonal extreme precipitation at the Paleocene–Eocene boundary. *Geology* 35:215–218
- Scholle PA, Ulmer-Scholle DS (2006) A Color Guide to the Petrography of Carbonate Rocks: grains, textures, porosity, diagenesis. AAPG, Tulsa, p 463
- Shinn EA (1983) Tidal flat environments. In: Scholle PA, Bebout DG, Moore CH (eds) Carbonate depositional environments Am Assoc of Petrol Geol Mem 33:172–210
- Sinclair HD, Sayer ZR, Tucker ME (1998) Carbonate sedimentation during early foreland basin subsidence: the Eocene succession of the French Alps. In: Wright VP, Burchette TP (eds) Carbonate ramps. *Geol Soc London Spec Publ* 149:205–227
- Spencer RJ, Lowenstein TK (1990) Evaporates. In: McIlreath IA, Morrow DW (eds) *Digenesis*. St. Johns, New Founland: Geosci. Canada Reprint Series 4, Geology Assoc. Canada, pp 141–163
- Stanly MS, Hardie LA (1998) Secular oscillations in the carbonate mineralogy of reef-building and sediment-producing organisms driven by tectonically forced shifts in seawater chemistry. *Palaeogeog Palaeoclimatol Palaeoecol* 144:3–19
- Tucker ME (1991) An introduction to the origin of sedimentary rocks. Blackwell, Science Publications, London, p 260
- Tucker ME, Wright VP (1990) Carbonate Sediment. Blackwells, Oxford 482
- Tucker ME, Calvet F, Hunt D (1993) Sequence stratigraphy of carbonate ramps: systems tracts, models and application to the Muschelkalk carbonate platform of eastern Spain. In: Posamentier HW, Summer CP, Haq BU, Allen GP (eds) Sequence stratigraphy and facies associations. *Int Assoc Sed Spec Publ* 18:397–415
- Vaziri-Moghaddam H, Kimiagari HM, Taheri A (2006) Depositional environment and sequence stratigraphy of the Oligocene–Miocene Asmari Formation in SW Iran. *Lali Area Facies* 52:41–51
- Veizer J (1983) Trace elements and isotopes in sedimentary carbonates. *Rev Mineral* 11:265–300
- Veizer J, Ala D, Azmy K, Bruckschen P, Buhl D, Bruhn F, Carden GAF, Diener A, Ebner S, Goddard Y, Jasper T, Korte C, Pawellek F, Podlaha OG, Strauss H (1999) $^{87}\text{Sr}/^{86}\text{Sr}$, $\delta^{13}\text{C}$ and $\delta^{18}\text{O}$ evolution of Phanerozoic seawater. *Chem Geol* 161:59–88
- Warren JK (2006) Evaporite: sediments, resources and hydrocarbons. Springer-Verlag, Berlin, p 1035
- Westphal H, Munneck A (2003) Limestone- marl alternations: a warm-water phenomenon? *Geol* 31:263–266
- White PD, Schiebout J (2008) Paleogene paleosols and changes in pedogenesis during the initial Eocene thermal maximum: Big Bend National Park Texas, USA. *GSA Bull* 120:1347–1362
- Wilkinson BH, Algeo TJ (1989) Sedimentary carbonate record of calcium–magnesium cycling. *Am Sci* 289:1158–1194
- Wilkinson BH, Owen RM, Carroll AR (1985) Submarine hydrothermal weathering, global eustasy, and carbonate polymorphism in Phanerozoic marine oolites. *J Sediment Petrol* 55:171–183
- Wilson MEJ, Vecsei A (2005) The apparent paradox of abundant foramol facies in low latitudes: their environmental significance and effect on platform development. *Earth Sci Rev* 69:133–168
- Winefield PR, Nelson CS, Hodder APW (1996) Discriminating temperate carbonates and their diagenetic environments using bulk elemental geochemistry: a reconnaissance study based on New Zealand Cenozoic limestones. *Carb Evap* 11:19–31
- Wright VP (1986) Facies sequences on a carbonate ramp: the Carboniferous limestone of South Wales. *Sedimentology* 33:221–241
- Zachos JC, Pagani M, Sloan L, Thomas E, Billups K (2001) Trends, rhythms, and aberrations in global climate 65 Ma to present. *Science* 292:686–693
- Zachos JC, Dickens GR, Zeebe RE (2008) An early Cenozoic perspective on greenhouse warming and carbon-cycle dynamics. *Nature (London, UK)* 451:279–283
- Zohdi A (2007) Geochemistry, diagenesis and sedimentary environment of the carbonate deposits of the Tale- Zang Formation in type section at Langar Anticline, (Dehluran), Iran (MSc thesis) Shahid Beheshti University, Iran, p 154